Nonlocal InSAR Filtering for DEM Generation and Addressing the Staircasing Effect

Gerald Baier, German Aerospace Center, gerald.baier@dlr.de, Germany
Xiao Xiang Zhu, German Aerospace Center & Technical University of Munich, xiao.zhu@dlr.de, Germany
Marie Lachaise, German Aerospace Center, marie.lachaise@dlr.de, Germany
Helko Breit, German Aerospace Center, helko.breit@dlr.de, Germany
Richard Bamler, German Aerospace Center & Technical University of Munich, richard.bamler@dlr.de, Germany

Abstract

A nonlocal InSAR filter is proposed that avoids the staircasing effect, which is especially troubling for DEM generation as it leads to terrace-like artifacts for hilly terrain. The sources of the staircasing effect for InSAR filtering are presented and the proposed filter is evaluated with simulations and test data, which show that the noise reduction and detail preservation are comparable to a state of the art nonlocal filter.

1 Introduction

The last years have seen a tremendous increase in globally available digital elevation data. Starting with the Shuttle Radar Topography Mission that made a global digital elevation model (DEM) with a resolution of $90\mathrm{m}\times90\mathrm{m}$, and recently $30\mathrm{m}\times30\mathrm{m}$ available, new DEM products with increasing resolutions have come on the market, such as Airbus' WorldDEM which relies on the TanDEM-X mission to produce a DEM with a $12\mathrm{m}\times12\mathrm{m}$ raster or ALOS World 3D which uses optical data from Jaxa's Advanced Land Observing Satellite to generate a globally available DEM of $5\mathrm{m}\times5\mathrm{m}$ resolution. These developments highlight the demand for globally available high resolution DEMs.

For synthetic aperture radar (SAR) sensors both range and azimuth resolution are inherently limited by physical constraints: system bandwidth and swath width (if still experimental techniques such as beam forming are not taken into account). As a result it is advisable that processing should not further compromise resolution, as is the case with many simple local filters.

This paper introduces an interferometric SAR (InSAR) filter based on the nonlocal concept called NLNOS for **N**on**L**ocal **NO S**taircase, which does not exhibit the staircasing effect for hilly terrain and retains the desired properties of nonlocal filters, i.e. noise reduction and detail preservation, with the goal of producing a final global DEM product using TanDEM-X data with so far unseen accuracy and resolution.

2 The Nonlocal Concept

The nonlocal filter was first introduced in [1]. Compared to simple neighborhood averaging filters, a nonlocal filter operates on a far larger area —hence the name —called the search window where it searches for similar pixels. The similarity is not only a function of the pixels, but also their surrounding areas, called patches, in order to take geometric structure into account, avoiding the so commonly seen smoothing of edges in traditional neighborhood filters. The similarities in the search window are mapped by an exponential kernel into weights and the final estimate $\hat{u}$ is given as the weighted mean over the search window:

$$\hat{u}(\mathbf{x}) = \sum_{\mathbf{y}\in\partial_{\mathbf{x}}} w(\mathbf{x},\mathbf{y})u(\mathbf{y}), \tag{1}$$

where w are the weights and $\partial_{\mathbf{x}}$ is the search window at the pixel location $\mathbf{x}$.

The filtering concept is illustrated by **Figure 1**, which depicts on the left how the similarities are computed between a center pixel (red) and all other pixels in the search window (blue) by comparing their patches (green) and the corresponding weight map on the right.

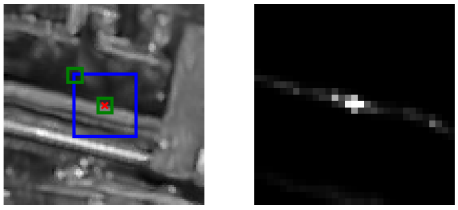

Figure 1: Nonlocal filtering concept (left) and weight map for the selected pixel (right)

The nonlocal filtering concept was adapted to InSAR and SAR noise statistics [2, 3], and later extended to a unified approach for (Pol)(In)SAR [4]. These filters are all capable of significantly reducing phase noise as well as preserving resolution, however at the cost of vast computational effort.

3 Nonlocal Filtering for DEM Generation

Due to their exceptional noise reduction and detail preservation nonlocal filters have piqued our interest for improving the resolution of the TanDEM-X DEM from $12\mathrm{m}\times12\mathrm{m}$, which relies on a simple boxcar averaging

filter, to 6m×6m. For our initial investigation we employed the NLInSAR filter, which is briefly introduced here. For a complete description the interested reader is referred to [2].
NLInSAR pursues a probabilistic approach for computing the similarities, meaning how probable is it that the reflectivity r, interferometric phase φ and coherence γ, i.e. the underlying parameters Θ_i of two pixels are identical, given the observed amplitudes and phase, i.e. the observations $\mathcal{O}_i$ for $i = 1, 2$:

$$p(\Theta_1 = \Theta_2 | \mathcal{O}_1, \mathcal{O}_2). \tag{2}$$

Employing Bayes' theorem yields:

$$\begin{aligned} p(\Theta_1 = \Theta_2 | \mathcal{O}_1, \mathcal{O}_2) \propto \\ p(\mathcal{O}_1, \mathcal{O}_2 | \Theta_1 = \Theta_2) \times p(\Theta_1 = \Theta_2), \end{aligned} \tag{3}$$

where $p(\mathcal{O}_1, \mathcal{O}_2 | \Theta_1 = \Theta_2)$ is the likelihood that the two observations stem from the same random process with parameters $\Theta_1 = \Theta_2$ and $p(\Theta_1 = \Theta_2)$ is a prior term to gauge the probability that $\Theta_1 = \Theta_2$. As these are in fact the parameters that have to be estimated, NLInSAR is an iterative algorithm that plugs in the previous estimate to compute $p(\Theta_1 = \Theta_2)$.
The similarities are mapped to weights with an exponential kernel and the final estimate for reflectivity $\hat{r}$, interferometric phase $\hat{\varphi}$, and coherence $\hat{\gamma}$ for a pixel $\mathbf{x}$ are given by:

$$\hat{r} = \frac{a}{N}, \qquad \hat{\varphi} = -\arg x, \qquad \hat{\gamma} = \frac{|x|}{a}, \tag{4}$$

with:

$$\begin{aligned} a &= \frac{1}{2} \sum_{\mathbf{y} \in \partial_{\mathbf{x}}} w(\mathbf{x}, \mathbf{y}) \left(A_m^2(\mathbf{y}) + A_s^2(\mathbf{y}) \right), \\ x &= \sum_{\mathbf{y} \in \partial_{\mathbf{x}}} w(\mathbf{x}, \mathbf{y}) A_m(\mathbf{y}) A_s(\mathbf{y}) e^{-j\phi(\mathbf{y})}, \\ N &= \sum_{\mathbf{y} \in \partial_{\mathbf{x}}} w(\mathbf{x}, \mathbf{y}), \end{aligned} \tag{5}$$

where A_m, A_s are the amplitudes of the master and slave images and ϕ is their interferometric phase.
While our initial investigation [5] with NLInSAR confirmed the aforementioned qualities of nonlocal filters, we observed terrace-like artifacts in mountainous regions as in **Figure 2**, which shows the DEMs produced by the standard boxcar filter and NLInSAR.

3.1 The Staircasing Effect

This phenomenon is an intrinsic problem of neighborhood and nonlocal filters [6], the reason is illustrated by **Figure 3**, which shows a convex nonlinear phase change and for a selected center pixel its search window and corresponding weight map.
Due to the nonlinear phase change pixels on the left of the center pixel have a phase which is closer to the center pixel's phase than pixels on the right, leading also to

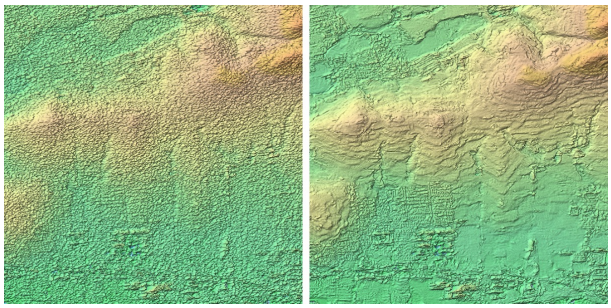

Figure 2: DEMs produced by a boxcar filter (left) and NLInSAR (right)

larger weights for these pixels. In order to get an unbiased phase estimate the weight map has to perfectly match the corresponding phase. As this is virtually impossible to hold for all pixels the phase estimate will be biased. When a convex region meets a concave region this bias will lead to the creation of staircases around the point of inflection.
An additional source for staircases is a bias in the weight map due to changes in amplitude that are not concurrent with changes in phase.
For conventional local filters this phenomenon is far less pronounced due to their far smaller windows.

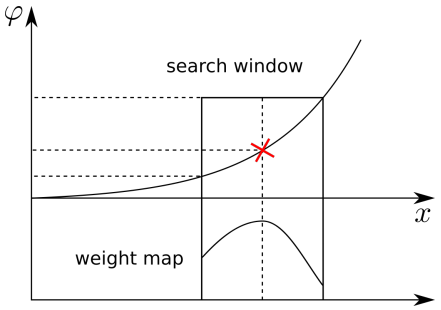

Figure 3: Nonlinear phase change and corresponding weight map

The staircasing effect is exacerbated for NLInSAR due to its iterative nature, as errors aggregate and aggravate through the prior term.

3.2 Proposed Solution

The solution presented in [6], although quite simplistic, efficiently removes occurring staircases in optical images and is adapted in our proposed filter to InSAR. In lieu of the conventional weighted means as in Equation (1), an estimate of the phase $\hat{u}$ is computed by fitting a plane through the complex phasor u defined by the interferometric phase, adjusted by the weights, and taking the plane's central value as an estimate:

$$\begin{aligned} \arg\min_{a,b,c} \sum_{\mathbf{y} \in \partial_{\mathbf{x}}} w(\mathbf{x}, \mathbf{y}) (a y_1 + b y_2 + c - u(\mathbf{y}))^2 \\ \hat{u}(\mathbf{x}) = a x_1 + b x_2 + c, \end{aligned} \tag{6}$$

where x_1, x_2 are the plane's center coordinates. We employed this scheme during the first iteration of NLInSAR

(i.e. without any prior) to obtain an estimate of the topographic phase, which is afterwards removed from the input data. All subsequent iterations of NLInSAR are executed as usual. At the end the topographic phase is added to the filtered interferometric phase. A flow graph diagram of our proposed modification to NLInSAR is depicted in **Figure 4**.

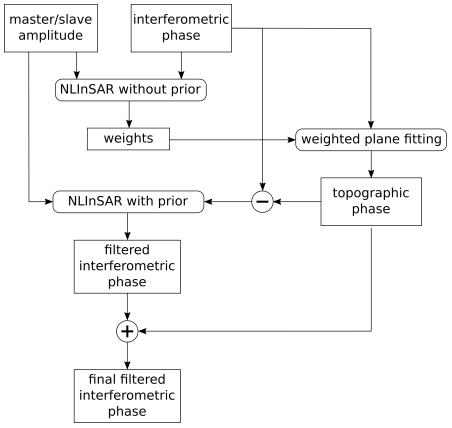

Figure 4: Flow graph of NLNOS

4 Simulation Results

A Monte-Carlo simulation for a nonlinear phase change was conducted for the classic NLInSAR filter and NLNOS, the result of which are shown in **Figure 5**. A comparatively large search window of size 31×31 was selected to make the staircasing effect more pronounced. The outcome shows that NLNOS is to a lesser degree affected by the staircasing effect than NLInSAR, which misestimates the interferometric phase around nonlinearities.

The root of this discrepancy in performance can be better understood by investigating NLInSAR's weight maps, which for selected points (marked by red dots) are plotted in the figure's lower part for the filter's last iteration and show that the staircase-like shape is a result of a skewed weight map. By fitting a plane through such a slanted weight map and the phase as in Equation (6) the plane's central pixel resembles the true value more closely than a simple weighted average.

In order to assess whether the detail preservation or noise reduction properties of NLInSAR are affected by the modifications of NLNOS a second Monte-Carlo simulation for a plateau in amplitude, phase and coherence with sharp edges was conducted. **Figure 6** shows the resulting interferometric phase estimates, for comparison the estimate obtained by a 7×7 boxcar filter is also plotted. Both nonlocal filters perform similarly, especially edges are not smoothed, however our proposed filter suffers from a slightly increased variance.

5 Experimental Results

A preliminary experiment with TanDEM-X data was conducted for a hilly test site in Southern Germany with agricultural fields, patches of forest and two gravel quarries. For validation a high resolution LiDAR digital terrain model (DTM) with $1\mathrm{m} \times 1\mathrm{m}$ raster, where vegetation and man-made structures are removed, was supplied by the *Bayerische Vermessungsverwaltung*.

NLNOS as well as NLInSAR were plugged into DLR's *Integrated TanDEM-X Processor* [7, 8] to generate a DEM for the test area. For comparison the DEM produced by the standardly employed boxcar filter was also computed. **Figure 7** shows the resulting DEMs as well as their differences to the LiDAR DTM in height, which are depicted again separately in the histogram in the top row. Height differences to the LiDAR DTM are observable for forested areas and some agricultural fields as electromagnetic waves at X-Band do not penetrate canopies. At the two gravel quarries the height estimates are also different, presumably caused by new excavations, as the LiDAR measurements were acquired roughly two years after the TanDEM-X data. These areas were excluded from our further analysis.

As is evident from the difference maps and the histogram both nonlocal filters produce a height estimate of lower variance than the boxcar filter, which is to be expected due to the in general far higher number of equivalent looks for each pixel. Also visible is the complete elimination of the staircasing effect when comparing the NLInSAR to the NLNOS estimate.

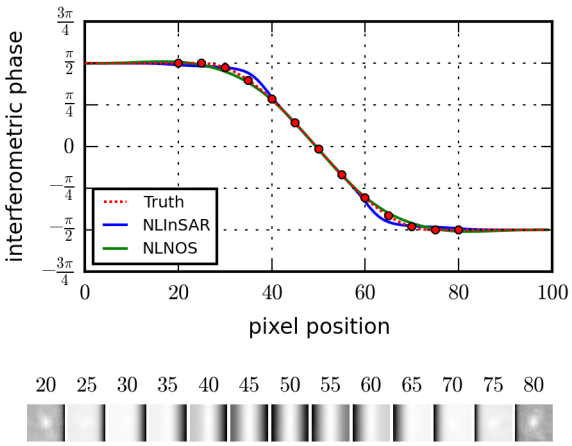

Figure 5: Results of a Monte-Carlo simulation for nonlinear phase and weight maps at selected pixels for NLInSAR

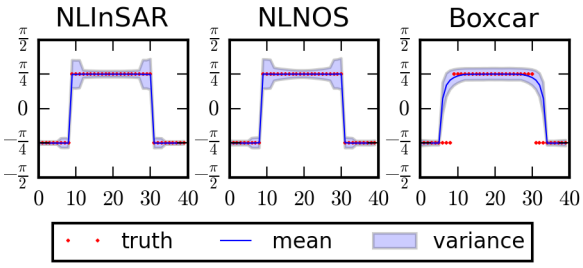

Figure 6: Monte-Carlo simulation for sudden steps in the phase image

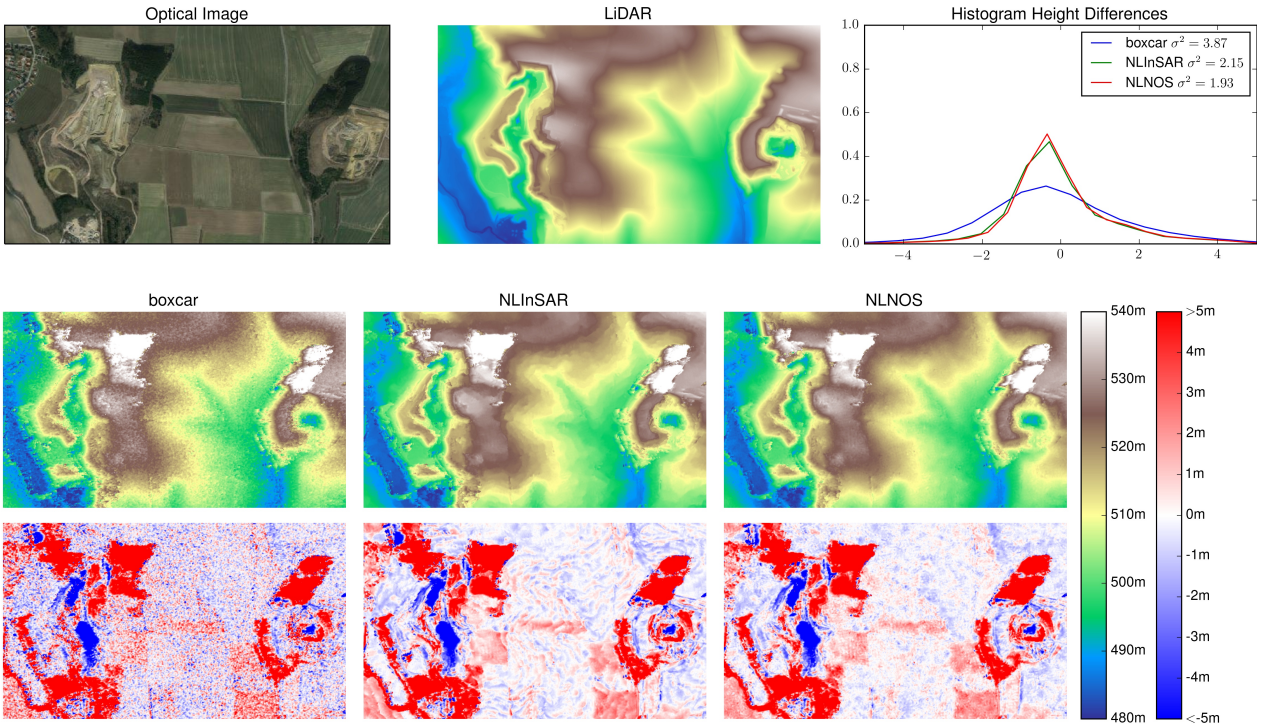

Figure 7: Top: optical image ©Google, LiDAR DTM ©Bayerische Vermessungsverwaltung, and histogram of the height differences with the LiDAR DTM; Bottom: DEMs produced by the boxcar, NLInSAR and NLNOS filters and their height differences to the LiDAR DTM

6 Conclusion

The appeal of employing nonlocal filtering prior to DEM generation was demonstrated. A nonlocal filter was presented which avoids the staircasing effect, inherent to neighborhood filters but which is exacerbated for nonlocal filters by their large search windows. The staircasing effect is especially undesired for generating DEMs as it results in terrace-like artifacts in hilly terrain. The proposed algorithm is a modification of the well known NLInSAR nonlocal filtering algorithm and keeps its level of noise reduction and detail preservation but does not exhibit its propensity for steps in the interferometric phase estimate.

Future work will focus on a more comprehensive evaluation of the accuracy and resolution of the produced DEMs.

References

[1] A. Buades, B. Coll, and J.-M. Morel, "A non-local algorithm for image denoising," in *IEEE Computer Society Conference on Computer Vision and Pattern Recognition, 2005. CVPR 2005*, vol. 2, pp. 60–65 vol. 2, June 2005.

[2] C.-A. Deledalle, L. Denis, and F. Tupin, "NL-InSAR: Nonlocal Interferogram Estimation," *IEEE Transactions on Geoscience and Remote Sensing*, vol. 49, pp. 1441–1452, Apr. 2011.

[3] S. Parrilli, M. Poderico, C. Angelino, and L. Verdoliva, "A Nonlocal SAR Image Denoising Algorithm Based on LLMMSE Wavelet Shrinkage," *IEEE Transactions on Geoscience and Remote Sensing*, vol. 50, pp. 606–616, Feb. 2012.

[4] C.-A. Deledalle, L. Denis, F. Tupin, A. Reigber, and M. Jäger, "NL-SAR: A Unified Nonlocal Framework for Resolution-Preserving (Pol)(In)SAR Denoising," *IEEE Transactions on Geoscience and Remote Sensing*, vol. 53, pp. 2021–2038, Apr. 2015.

[5] X. X. Zhu, R. Bamler, M. Lachaise, F. Adam, Y. Shi, and M. Eineder, "Improving TanDEM-X DEMs by Non-local InSAR Filtering," in *EUSAR 2014; 10th European Conference on Synthetic Aperture Radar; Proceedings of*, pp. 1–4, June 2014.

[6] A. Buades, B. Coll, and J.-M. Morel, "The staircasing effect in neighborhood filters and its solution," *IEEE Transactions on Image Processing*, vol. 15, pp. 1499–1505, June 2006.

[7] T. Fritz, C. Rossi, N. Yague-Martinez, F. Rodriguez-Gonzalez, M. Lachaise, and H. Breit, "Interferometric processing of TanDEM-X data," in *Geoscience and Remote Sensing Symposium (IGARSS), 2011 IEEE International*, pp. 2428–2431, July 2011.

[8] H. Breit, T. Fritz, U. Balss, A. Niedermeier, M. Eineder, N. Yague-Martinez, and C. Rossi, "Processing of bistatic TanDEM-X data," in *Geoscience and Remote Sensing Symposium (IGARSS), 2010 IEEE International*, pp. 2640–2643, July 2010.